Available online at www.sciencedirect.com
ScienceDirect
Trans. Nonferrous Met. Soc. China 31(2021) 3879−3890

Transactions of Nonferrous Metals Society of China
www.tnmsc.cn

Flotation separation of molybdenite and talc using tragacanth gum as depressant and potassium butyl xanthate as collector

Chun-hui ZHONG[1], Bo FENG[1,2,3], Yuan-gan CHEN[1], Meng-chi GUO[1], Hui-hui WANG[1]

1. Jiangxi Key Laboratory of Mining Engineering,
Jiangxi University of Science and Technology, Ganzhou 341000, China;
2. State Key Laboratory of Mineral Processing, BGRIMM Technology Group, Beijing 102628, China;
3. Key Laboratory of Hunan Province for Clean and Efficient Utilization of Strategic Calcium-containing
Mineral Resources, Central South University, Changsha 410083, China

Received 4 January 2021; accepted 26 August 2021

Abstract: Tragacanth gum (TG) was explored as a depressant to realize the flotation separation of molybdenite and talc. The flotation experiments indicated that when using potassium butyl xanthate (PBX) as a collector, molybdenite showed excellent floatability while talc was completely depressed by TG, thus realizing the flotation separation of the two minerals. X-ray photoelectron spectroscopy (XPS) analysis results showed that TG was adsorbed on molybdenite surface via chemisorption. The results of contact angle measurement, Fourier transform infrared (FTIR) spectroscopy, and time-of-flight secondary ion mass spectrometry (ToF-SIMS) indicated that the pre-adsorption of TG on molybdenite could not hinder the further chemisorption of PBX on molybdenite. Because PBX has no collecting ability on talc, the flotation separation of molybdenite and talc came true using PBX to collect molybdenite and TG to depress talc.

Key words: molybdenite; tragacanth gum; organic depressant; talc; flotation separation

1 Introduction

Talc is common magnesium-containing layered silicate mineral, which is easy to enter the molybdenum concentrate along with the molybdenite flotation due to its good natural hydrophobicity. The residue of talc in molybdenum concentrate leads to the decrease of concentrate quality, and the increase in the content of magnesium in the molybdenum concentrate causes the slag to be sticky and the melting point to increase, which can increase the cost of the next smelting process [1−5]. Therefore, the effective separation and removal of talc from molybdenite can not only improve the efficiency of resource utilization, but also reduce the production cost, which is a research hotspot and a challenge at present.

In the flotation separation of sulphide ore containing talc, there are generally three ways in view of talc's good floatability: pre-flotation to removal talc, inhibiting talc while floating sulfide ore, and removing talc from mixed concentrate by acid leaching [6−10]. When using pre-flotation method to removal talc, the amount of talc removal and the dosage of reagent are hard to control. Moreover, removing talc from mixed concentrate by acid leaching requires a large amount of acid solution and it is harmful to equipment, so this method is also rarely used. Therefore, the direct flotation of molybdenite is a more effective and environment-friendly method, and the development of effective talc inhibitors in the flotation process of molybdenite is the key to realize this aim [11,12].

Over the last few decades, many depressants

Corresponding author: Bo FENG, Tel: +86-18270767369, E-mail: fengbo319@163.com

DOI: 10.1016/S1003-6326(21)65771-0

have been exploited to inhibit the flotation of talc including inorganic (e.g., Na_2SiO_3, Na_2CO_3, $ZnSO_4$, and $Al_2(SO_4)_3$) [1,13] and organic depressants (e.g., carboxymethyl cellulose (CMC), guar gum, humic substances, and starch) [3,13−19] as well as the combinations of them. Although the above-mentioned reagents have achieved a certain extent of success in the depression of talc, their practical applications are subjected to the toxicity and high price. Therefore, it is urgent to develop more efficient and environmentally friendly talc inhibitors, and the relative mechanism investigation will contribute to such a process.

Tragacanth gum (TG) is a white or yellow-white powder, which is a natural gum obtained from the dried juice of legumes. A viscous colloidal solution is formed after being dissolved in water and can be used as emulsifier, lubricating agent, adhesives agent and suspending agent in the medicine and food industry [20]. We used TG in the previous study as a depressant of talc during the chalcopyrite flotation and achieved effective separation of the two minerals. In addition, according to zeta potential and XPS measurements results, we speculated that TG was adsorbed on talc surface mainly through physical interactions, hydrophobic interaction was considered as the main driving force and hydrogen bond may also play a role. However, there is less report on the influence of TG on flotation behavior of molybdenite and whether TG can separate it and talc is still unknown. Therefore, this study is aimed at evaluating the possibility of flotation separation of molybdenite and talc by TG, and the experiments were conducted in the flotation system with PBX as a collector instead of traditionally used kerosene. In addition, the adsorption mechanism of TG on molybdenite surface was explored by XPS technology with the competitive adsorption relationship of PBX and TG on molybdenite surface being fully discussed by contact angle measurement, FTIR spectroscopy, and ToF-SIMS determination. This study will provide an interesting idea for exploring effective depressants in flotation separation of sulfides and silicate minerals.

2 Experimental

2.1 Samples and reagents

Molybdenite and talc lumps of high purity were obtained from Guangzhou, China. After manual crushing, impurities removal, agate grinding and dry screening, the obtained 37−150 μm size fractions were used for flotation experiments, XPS analysis, and ToF-SIMS determination, and the <37 μm particles were prepared for FTIR spectroscopy test. The results of XRD analysis (Fig. 1) and chemical analysis (Table 1) showed that molybdenite and talc were of high purity of 95.46% and 95.73% respectively.

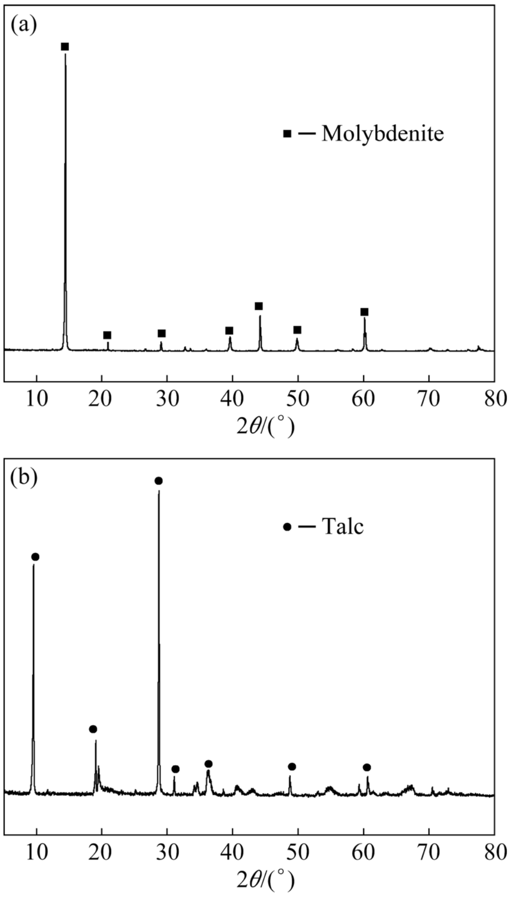

Fig. 1 XRD patterns of molybdenite (a) and talc (b)

Table 1 Chemical composition of molybdenite and talc (wt.%)

Sample	Mo	Fe	MgO	SiO_2	Purity
Molybdenite	57.22	−	−	−	95.46
Talc	−	0.56	30.39	63.05	95.73

Reagents used in this study include collector PBX, depressant TG (Fig. 2), frother methyl isobutyl carbinol (MIBC) and pH regulators of hydrochloric acid (HCl) and sodium hydroxide (NaOH). PBX was of industrial grade and it was obtained from Nanjing Yinmao lead-zinc mine. The rest reagents were of analytical grade and they were purchased from Shanghai Macklin Biochemical Co., Ltd. The flotation experiments were conducted in distilled water with a resistivity of 18.2 MΩ·cm. Figure 2 shows that hydroxyl and carboxylthe are the main function groups in molecular structure of TG.

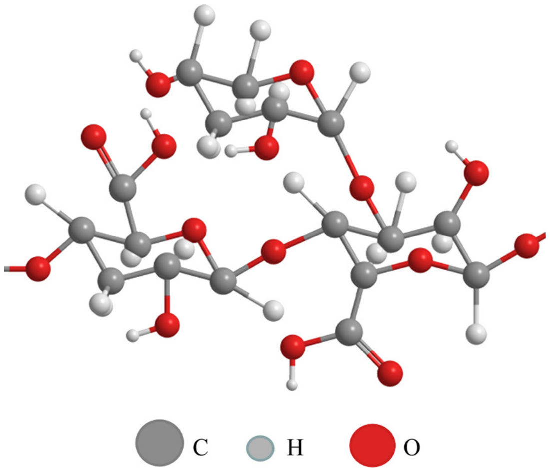

Fig. 2 Molecular structure of TG [20]

2.2 Flotation tests

In the single mineral flotation experiment, mineral samples were added to the XFGII5 hanging trough flotation machine (Changchun, China), and the spindle speed was set to be 1992 r/min. The flotation flowsheet was as follows: 2 g of samples were mixed with 40 mL of distilled water and the slurry pH was adjusted with HCl or NaOH. After 3 min conditioning, TG, PBX and MIBC were added in sequence with 3 min conditioning time respectively. After 3 min flotation, the obtained flotation products were filtered, dried and weighed sequentially to calculate the recovery. In the mixed minerals flotation experiment, Mo grade in the flotation products was analyzed for recovery calculation.

2.3 XPS analysis

The 1 g of molybdenite sample was mixed with 25 mg/L TG solution at pH 9. After conditioning for 10 min, the solid−liquid separation was conducted. The filtered solid mineral was dried in a vacuum drying oven below 40 °C. XPS analysis was conducted with an X-ray photoelectron spectrometer (Thermo Scientific Escalab 250Xi, USA).

2.4 Contact angle measurement

The polished sample blocks were soaked in a breaker containing 50 mg/L TG and 2.0×10^{-4} PBX solutions for 10 min. The samples were then washed three times with distilled water and then dried with nitrogen. The contact angle was measured three times for each sample using a SL200C contact angle instrument (Shanghai, China), and the mean value was used as the result.

2.5 FTIR spectroscopy

The FTIR spectra test was conducted with an ALPHA FTIR spectrometer (Bruker, Germany). Firstly, the sample was ground to particle size of <37 μm, and then 1 g sample and 40 mL distilled water were mixed in a beaker. After the pulp pH was adjusted to be 9, a desired concentration of TG solution was added. After stirring for 10 min, the solid−liquid separation was conducted, and the obtained mineral was washed three times with distilled water, followed by drying in a vacuum drying oven below 40 °C before FTIR spectroscopy test.

2.6 ToF-SIMS analysis

The adsorption and distribution of TG and PBX on molybdenite surface were investigated by time-of-flight secondary ion mass spectrometry (ToF-SIMS) (ION-ToF, Munster, Germany). Surface analysis was carried out with Bi^{3+} with energy of 30 kV as the primary ion and an analysis current of 0.95 pA. The area of the sample used for surface analysis was 500 μm × 500 μm. The negative secondary ion mass spectra were calibrated with CH^-, CH_2^- and CH_3^-.

3 Results and discussion

3.1 Flotation experiment result

Molybdenite and talc are minerals with natural floatability and they can float under the condition of only adding frother. As seen from Fig. 3(a), at pH=9, the flotation recoveries of molybdenite and talc were 88.55% and 89.05%, respectively, in the flotation system with frother alone. To reduce the interference of other reagents when discussing the effects of one reagent, the effect of TG on the molybdenite and talc flotation was investigated under the condition of no collector. As can be seen in Fig. 3(a), when 25 mg/L TG was added into flotation pulp, both molybdenite and talc were completely depressed, illustrating the strong depressive effect of TG on the two minerals. Figure 3(b) shows the influence of pH on the depressive effect of TG on molybdenite and talc. The results indicated that TG can completely depress the flotation of molybdenite and talc at pH of 3−11, reflecting its extensive applicability.

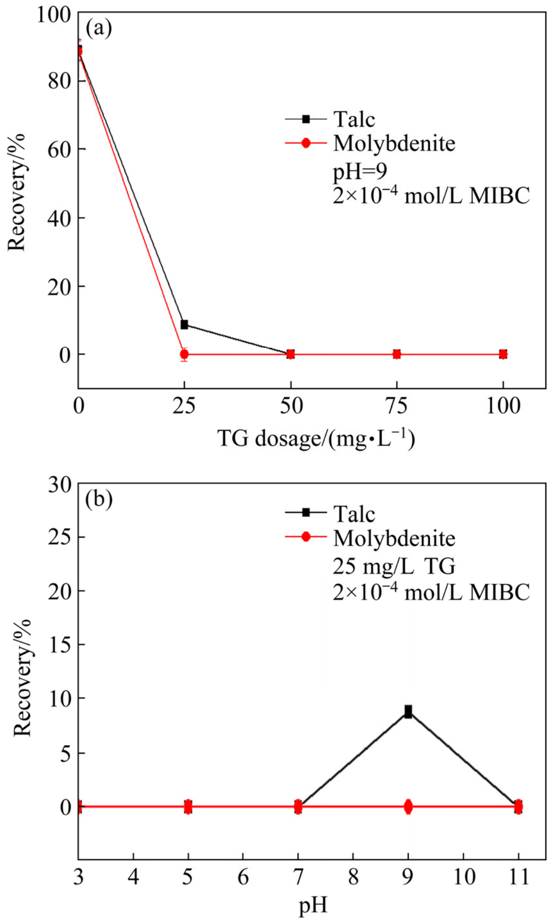

Fig. 3 Effect of TG on flotation of molybdenite and talc at different TG dosages (a) and pH values (b)

The results of Fig. 3 showed that both molybdenite and talc were depressed by TG, and thus one of them must be activated by a collector to achieve their flotation separation. It is universally known that PBX is a widely used sulfide mineral collector without collection on silicate minerals. Besides, it has been proven in practice that adding some polar collectors such as xanthate in the flotation of molybdenite is beneficial to the flotation [21−24]. Sequentially, the effect of PBX on the flotation of TG-treated molybdenite and talc was investigated. As depicted in Fig. 4(a), when PBX dosage increased from 0 to 1.0×10^{-4} mol/L, the flotation recovery of molybdenite increased sharply from 0 to 89.7%. With increasing the PBX dosage to 2.0×10^{-4} mol/L, the flotation recovery of molybdenite continued to increase to 93.8%, illustrating that molybdenite pre-inhibited by TG could be activated by PBX and had excellent floatability. In stark contrast, talc was always completely depressed by TG regardless of collector dosage.

Figure 4(b) shows the effect of PBX on the flotation of molybdenite and talc at various pH values. As shown in Fig. 4(b), pH had no influence on the depression effect of TG on talc. At pH 3−9, the flotation recovery of molybdenite remained above 90%, and it was slightly lower at pH=11, attributing to the oxidation of molybdenite under alkaline conditions. On account of the above results, TG can inhibit both molybdenite and talc. The difference is that after PBX was used, molybdenite can restore its original floatability while talc was still inhibited completely by TG, which provided a possibility for the flotation separation of the two minerals.

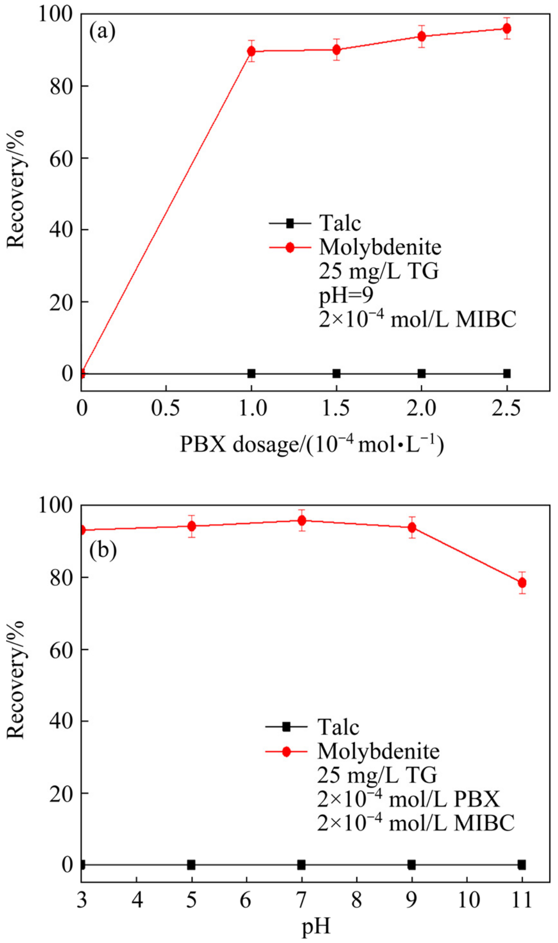

Fig. 4 Effect of PBX on flotation of molybdenite and talc at different PBX dosages (a) and pH values (b)

The flotation experiment of artificial molybdenite−talc mixtures was carried out to investigate the depressive effect of TG on talc and the collective effect of PBX on molybdenite. It can be seen from Table 2, at pH 9, a molybdenum concentrate with molybdenite recovery of 96.52% and Mo grade of 32.67% was obtained in the absence of depressant. The high yield and low Mo grade indicated that when molybdenite was collected, a major of talc also floated into concentrate. When 50 mg/L TG was added, a molybdenum concentrate with molybdenite recovery of 84.42% and Mo grade of 46.05% was obtained. By contrast, molybdenite recovery decreased by 12.1% while Mo grade increased by 13.38%, indicating that most of talc was depressed during molybdenite flotation.

Table 2 Flotation results for mixed minerals (1:1 mass ratio of molybdenite to talc) in absence and presence of depressant TG at pH 9 (2.0×10^{-4} mol/L PBX, and 2.0×10^{-4} mol/L MIBC)

Depressant	Product	Yield/%	Mo grade/%	Molybdenite recovery/%
50 mg/L TG	Concentrate	52.45	46.05	84.42
	Tailings	47.55	9.37	15.58
	Feed	100.00	28.61	100.00
None	Concentrate	85.00	32.67	96.52
	Tailings	15.00	6.67	3.48
	Feed	100.00	28.77	100.00

3.2 Adsorption mechanism of TG on molybdenite surface

The results of Fig. 3 showed that both molybdenite and talc were depressed by TG, inferring the adsorption of TG on the surfaces of two minerals. In previous research, we explored the adsorption mechanism of TG on talc surface through zeta potential and XPS measurements and speculated that TG was adsorbed on talc surface mainly through physical interactions. Among them, hydrophobic interaction, i.e., the behavior of two hydrophobic species coming together to avoid the water, was considered as the main driving force and hydrogen bond may also play a role [25]. However, the adsorption mechanism of TG on molybdenite surface remains unknown. Hence, in this study, we focused on the adsorption of TG on molybdenite surface and the competitive adsorption relationship between TG and PBX on molybdenite surface.

X-ray photoelectron spectroscopy (XPS) is often used in flotation studies to reveal the action mechanism between organic molecules and mineral surfaces. Hence, the XPS spectra of molybdenite before and after TG treatment were first determined and the corresponding results are shown in Fig. 5. From Fig. 5, the elements on molybdenite surface were the same before and after the addition of TG, including Mo, S, C and O, but atomic concentrations were changed. Specifically, the concentrations of Mo, S, C and O on bare molybdenite surface were 20.82, 37.68, 28.39 and 13.1 at.%, respectively. After TG addition, the concentrations of Mo and S decreased to 15.56 and 32.12 at.%, while the concentrations of C and O increased to 38.68 and 13.64 at.%, respectively, which supported the adsorption of TG on molybdenite surface.

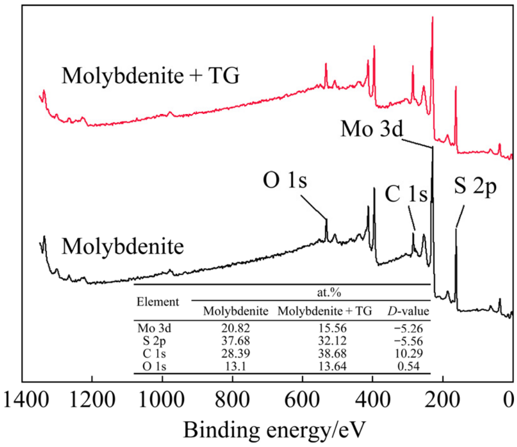

Fig. 5 XPS survey spectra for molybdenite before and after TG treatment

Figure 6 shows the XPS narrow scanning spectra of C 1s, O 1s, Mo 3d, S 2p of molybdenite before and after TG treatment to further reveal the chemical state of each element. From Fig. 6(a), the peak fitting of the C 1s for bare molybdenite gave one peak at 284.80 eV attributing to the C—C adventitious carbon contamination. After the addition of TG, two new peaks appeared at 286.63 and 288.76 eV, which came from C—O and C═O [26−28]. The fitted O 1s spectra before or after TG treatment only gave one peak at 532.51 or 532.58 eV, which was contributed to C—O (Fig. 6(b)). In the fitted Mo 3d spectra for bare molybdenite, the peak at 299.64 eV was assigned as MoS_2, while the other at 226.49 eV was related to

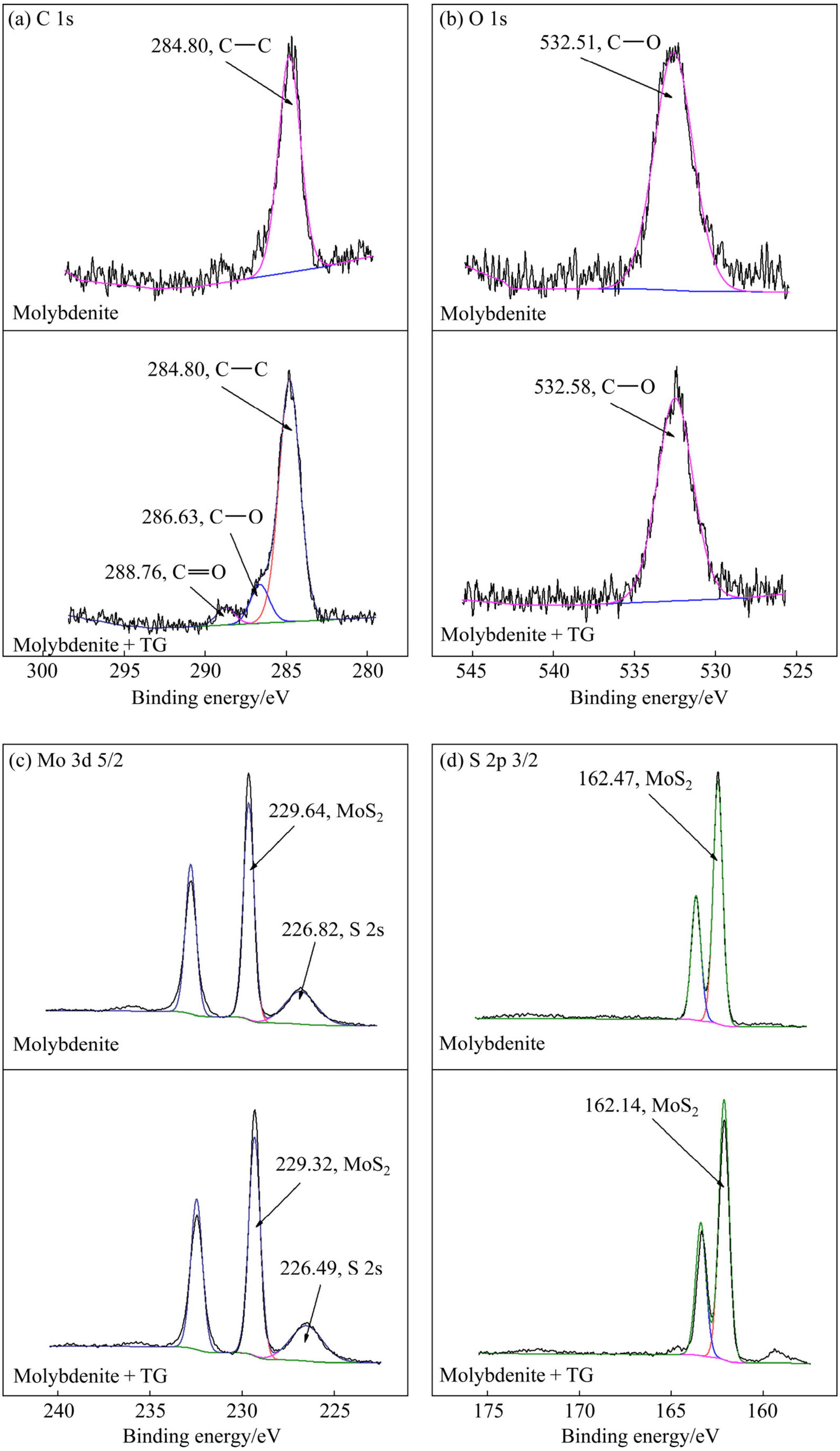

Fig. 6 XPS narrow scanning spectra of C 1s (a), O 1s (b), Mo 3d (c), and S 2p (d) of molybdenite before and after TG treatment

S 2s, whose region strongly overlaps Mo 3d region. It is worth noting that after TG addition, the binding energy of Mo 3d of MoS_2 moved to 229.32 eV, inferring the changing of electron density on Mo atoms. Similar changes could be also found from fitted S 2p spectra before and after TG treatment (i.e., decreasing from 162.47 to 162.14 eV, Fig. 6(d)). All of the above findings suggested that TG was adsorbed on molybdenite surface by chemisorption.

3.3 Competitive adsorption mechanism of PBX and TG on molybdenite surface

3.3.1 Contact angle measurement result

The flotation results showed that PBX and TG had competitive adsorption on the surface of molybdenite, and the adsorption capacity of PBX on the surface of molybdenite was stronger than that of TG on the surface of molybdenite. Therefore, PBX can replace the adsorbed TG molecules on the surface of molybdenite to some extent. The contact angle measurement, FTIR spectroscopy, and ToF-SIMS were conducted to prove it. It can be seen from Fig. 7 that the surface contact angle of bare molybdenite was 54.8°, which was similar to that reported in previous literatures [29−31]. At this point, molybdenite had a good floatability as proven in the single mineral flotation experiment. After treatment with TG, the contact angle of molybdenite decreased to 38.5°, indicating the adsorption of TG on the surface of molybdenite. After the TG-treated mineral was then treated by PBX, the contact angle of molybdenite increased to 62.5°, stating the further adsorption of PBX on the TG-treated molybdenite surface.

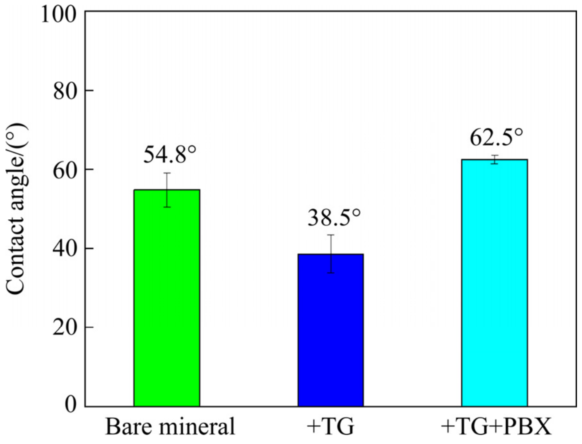

Fig. 7 Contact angles of molybdenite before and after treatment with TG and PBX

3.3.2 FTIR analysis

The FTIR spectra of molybdenite before and after TG and PBX treatment were measured. Firstly, the FTIR spectra of reagents TG and PBX were measured to determine the major functional groups in reagents molecular. As seen from Fig. 8(a), four kinds of peaks can be distinguished in the tested TG sample. It has been well documented that the absorption band at 3392 cm^{-1} is related to the hydroxyl (—OH) while the bands over ranges of 1416−2149 cm^{-1} are attributed to carbonyl (C═O) groups. The absorption peak at 2929 cm^{-1} corresponds to the vibration of —CH_2 groups, while that at 1026 cm^{-1} was indicated as clues for stretching vibrations of polyol carbonyl (C—O), ether and alcoholic groups [32−35]. As for PBX, four kinds of peaks can be identified in the tested sample. Among them, the absorption peak at 3401 cm^{-1} is ascribed to the vibration of hydroxyl (—OH), which comes from the moisture absorbed by PBX. The absorption peaks at 2960, 2934 and 2872 cm^{-1} correspond to the stretching vibration of —CH_3, —CH_2 and —CH groups, while those

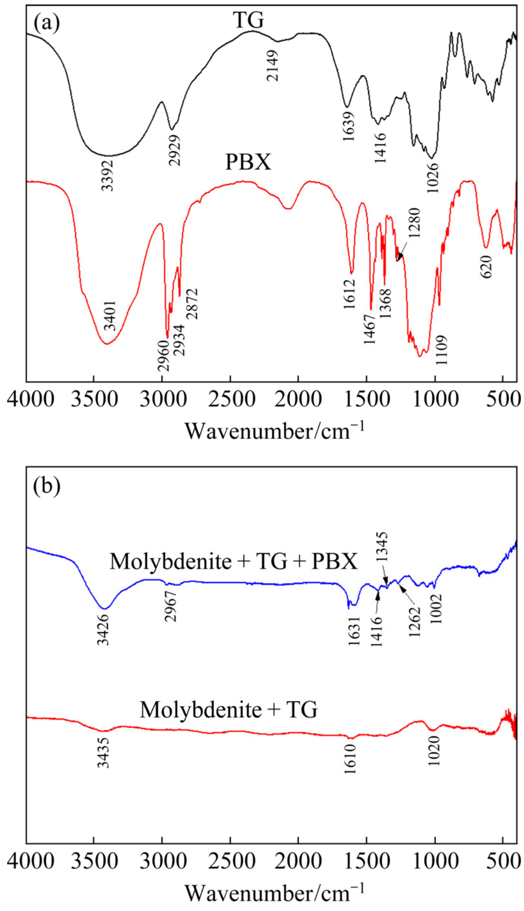

Fig. 8 FTIR spectra of TG and PBX (a), and molybdenite before and after reagents addition (b)

located at 1612, 1467, 1368 and 620 cm^{-1} are in connection with the deformation vibration of —CH_3, —CH_2 and —CH groups. The absorption peaks over the range of 1109−1280 cm^{-1} are attributed to the stretching vibration of C—O, C—S and C═S [36].

The FTIR spectra of molybdenite before and after treatment with TG and PBX are shown in Fig. 8(b). In the FTIR spectra of molybdenite with TG treatment, the possible absorption peaks of TG were seen on molybdenite surface at around 3435, 1610 and 1020 cm^{-1}, attributed to the stretching vibration of —OH, C═O and C—O respectively, validating the contact angle measurement and single mineral flotation experiment results that TG was adsorbed on molybdenite surface and inhibited its flotation.

When PBX was used, the possible absorption peaks of PBX appeared on molybdenite surface at around 2967, 1631, 1416, 1345 and 1262−1002 cm^{-1} corresponding to the stretching vibration of —CH_3, deformation vibration of —CH_3, —CH_2 and —CH groups and stretching vibration of C—O, C—S and C═S, respectively, indicating the adsorption of PBX on molybdenite surface. This demonstrated that the pre-adsorption of TG on molybdenite surface could not hinder the further adsorption of PBX. These were in good agreement with the contact angle measurement and the single mineral flotation experiment results that the pre-inhibited molybdenite by TG could obtain excellent floatability after the interaction with PBX.

3.3.3 ToF-SIMS analysis

The chemical statement of molybdenite surface after interaction with TG or TG+PBX can be detected by ToF-SIMS. In this study, ToF-SIMS measurement was conducted to determine the chemical composition of molybdenite concentrate and tailings surfaces. And the negative-ion ToF-SIMS spectra and images were selected to characterize the reagents adsorption on molybdenite surface.

In negative-ion spectra of molybdenite tailings obtained by TG treatment alone (Figs. 9(a, b)), the ions detected in the *m/z* range of 0−200 were O^- (*m/z* 16), OH^- (*m/z* 17), CH_2^- (*m/z* 25), S^- (*m/z* 32), C_2HO^- (*m/z* 41), CHO_2^- (*m/z* 45), $C_2H_3O_2^-$ (*m/z* 59), $C_3H_3O_2^-$ (*m/z* 71), $C_3H_3O_2^-$ (*m/z* 87), SO_4H^- (*m/z* 97), $C_4H_9OCS_2^-$ (*m/z* 149), and MoS_3^- (*m/z* 193), indicating the adsorption of organic molecule TG on molybdenite surface. It is noted that the ion intensities of O^- (*m/z* 16), OH^- (*m/z* 17), CH_2^- (*m/z* 25), C_2HO^- (*m/z* 41), CHO_2^- (*m/z* 45), $C_2H_3O_2^-$ (*m/z* 59), $C_3H_3O_2^-$ (*m/z* 71) and $C_3H_3O_3^-$ (*m/z* 87) on the molybdenite concentrate obtained by TG + PBX treatment were lower, while the ion intensities of S^- (*m/z* 32), $C_4H_9OCS_2^-$ (*m/z* 149), and MoS_3^- (*m/z* 193) were higher (Figs. 9(c, d)), compared with those on the molybdente tailings obtained by only TG treatment. More specifically, normalized intensities (NI) of OH^- (*m/z* 17) and CHO_2^- (*m/z* 45) on molybdenite tailings were 1.21×10^{-2} and 2.00×10^{-2}, respectively, while normalized intensity (NI) of $C_4H_9OCS_2^-$ (*m/z* 149) was 6.81×10^{-4}. It was noteworthy that OH^- (*m/z* 17) and CHO_2^- (*m/z* 45) represented the adsorption of TG, while $C_4H_9OCS_2^-$ (*m/z* 149) represented the adsorption of PBX. On molybdenite concentrate obtained by TG+PBX treatment, normalized intensities (NI) of OH^- (*m/z* 17) and CHO_2^- (*m/z* 45) were 8.38×10^{-3} and 9.97×10^{-3}, respectively, lower than those on molybdenite tailings obtained by only TG treatment; normalized intensity (NI) of $C_4H_9OCS_2^-$ (*m/z* 149) was 1.08×10^{-3}, higher than that on molybdenite tailings obtained by only TG treatment. The results of ToF-SIMS suggested that in the flotation system with TG and PBX, TG and PBX competed to adsorb on the surface of molybdenite, and the pre-adsorption of TG molybdenite surface could not hinder the further adsorption of PBX onto it.

3.4 Discussion

Molybdenite and talc are naturally floatable minerals and the two minerals have high flotation recovery with the addition of proper frother. TG has a heterpolar molecule with a large number of polar groups on the hydrocarbon skeleton, with hydroxyl and carboxyl groups throughout the molecule. When TG is added to the flotation pulp, part of the hydroxyl group and carboxyl group in TG molecules interact with molybdenite and talc surface through hydrogen bonding, hydrophobic interaction or chemical action, while the other polar groups move outward to form a hydrophilic adsorption layer, which enhances the hydrophilicity of the mineral surface.

PBX has a heteropoly molecule, which is composed of hydrophobic butyl group and hydrophilic xanthic acid group. According to the principle of “similarity attracts”, PBX has selective

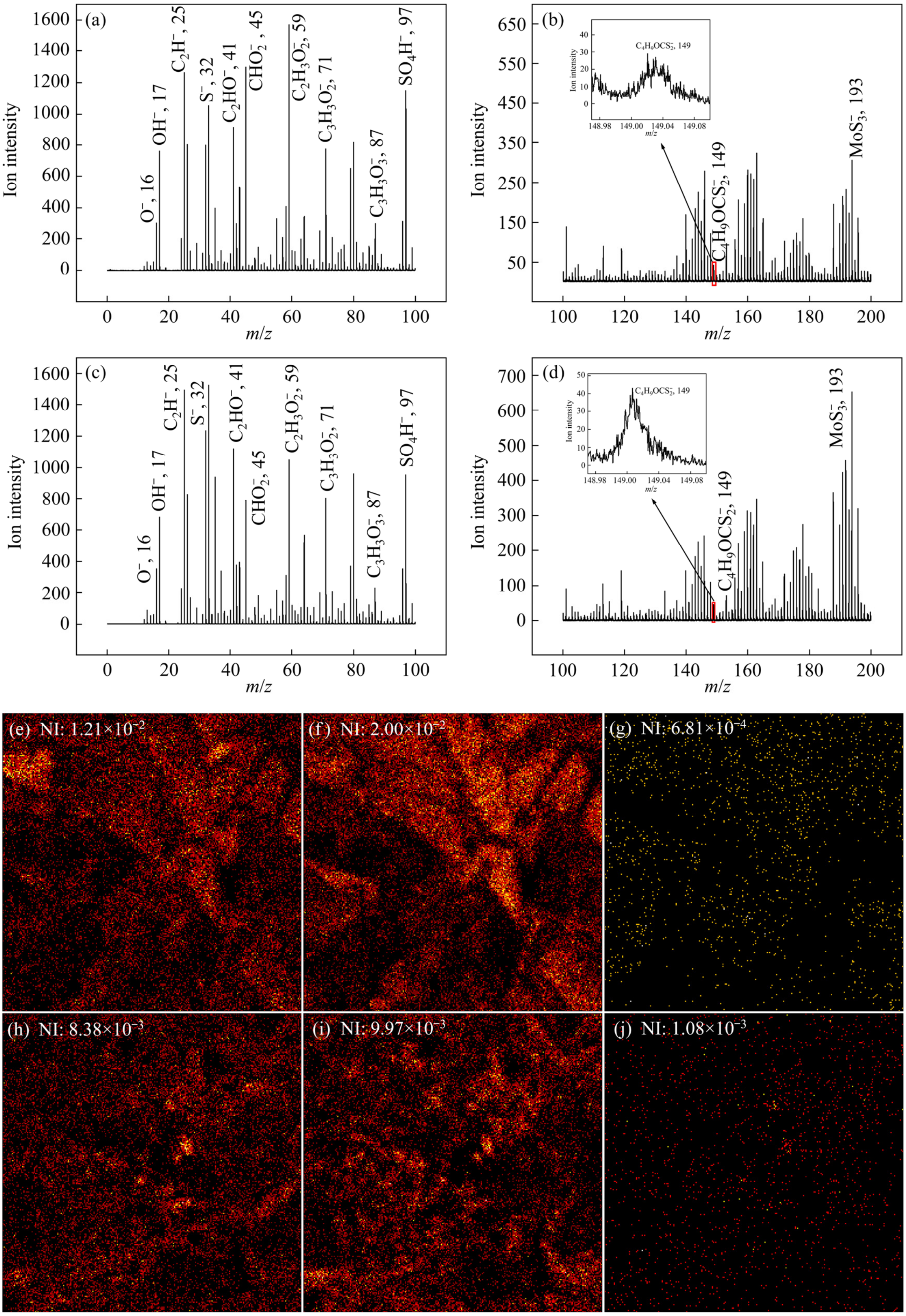

Fig. 9 Negative-ion ToF-SIMS spectra (a−d) and images (e−j) of surface of molybdenite tailings obtained by TG treatment alone (a, b, e, f, g) and molybdenite concentrates obtained by TG + PBX treatment (c, d, h, i, j)

collection effect on sulfide minerals containing S atoms on the mineral lattice surface. Molybdenite has a layered structure with two orientation surfaces: basal and edge planes. The basal planes are formed by the breakage of weak van der Waals forces between layers (S—S bonds) while the edge planes are generated by the rupture of strong covalent Mo—S bonds. WEI and LI [22] explored the reasons for the differences in the properties of molybdenite “surface” and “edge” through density functional theory and discussed the effects of water, kerosene, and xanthate on the surface of molybdenite. They found that the adsorption energy of PBX on the molybdenite “surface” is positive, while the adsorption energy on the molybdenite “edge” is negative, indicating that PBX can be adsorbed on the molybdenite “edge”, but cannot be adsorbed on the molybdenite “surface”, and PBX is adsorbed on molybdenum “edge” by the bonding interaction of the S atom in its C—S single bond with Mo atom at the molybdenite “edge”, which is consistent with the results of previous studies [21,23].

The polar xanthic acid of PBX can be adsorbed firmly on the surface of molybdenite, while the hydrophobic butyl group is arranged directionally outward, which causes the hydrophobic surface of molybdenite. The results of contact angle test, FTIR measurement and ToF-SIMS analysis show that in the flotation system containing TG and PBX, TG and PBX had competitive adsorption on the surface of molybdenite, and the pre-adsorption of TG on molybdenite could not hinder the subsequent adsorption of PBX on the surface of molybdenite. Therefore, as shown in the flotation results, molybdenite maintained a high flotation recovery, while the flotation of talc was seriously inhibited by TG, thus achieving the flotation separation of the two minerals.

4 Conclusions

(1) TG was a non-toxic, environmentally friendly and highly efficient organic depressant of molybdenite and talc and could completely depress the flotation of the two minerals in the absence of collector.

(2) In the flotation system consisting of TG and PBX, molybdenite showed excellent floatability while talc was severely depressed and the flotation separation of the two minerals was verified successful by artificial mixed minerals flotation experiment.

(3) XPS analysis show that TG was adsorbed on molybdenite surface by chemisorption, and meanwhile hydrogen bonding and hydrophobic interaction may also play a role in the adsorption process. The results of contact angle test, FTIR measurement and ToF-SIMS analysis showed that in the flotation system containing TG and PBX, TG and PBX had competitive adsorption on the surface of molybdenite, and the pre-adsorption of TG on molybdenite could not hinder the subsequent adsorption of PBX on the surface of molybdenite.

Acknowledgments

The authors are grateful for the financial supports from the National Natural Science Foundation of China (No. 51664020), the Natural Science Foundation of Jiangxi Province, China (No. 20202ACBL214010), Open Foundation of State Key Laboratory of Mineral Processing, China (No. BGRIMM-KJSKL-2020-12), and Open Foundation of Key Laboratory of Hunan Province for Clean and Efficient Utilization of Strategic Calcium-containing Mineral Resources, China (No. 2018TP1002).

References

[1] YUAN Duo-wei, XIE Lei, SHI Xing-wei, YI Long-sheng, ZHANG Guo-fan, ZHANG Hao, LIU Qi, ZENG Hong-bo. Selective flotation separation of molybdenite and talc by humic substances [J]. Minerals Engineering, 2018, 117: 34−41.

[2] FENG Bo, PENG Jin-xiu, ZHANG Wen-pu, NING Xiang-han, GUO Yu-tao, ZHANG Wen-cai. Use of locust bean gum in flotation separation of chalcopyrite and talc [J]. Minerals Engineering, 2018, 122: 79−83.

[3] ALLISON S A, O'CONNOR C T. An investigation into the flotation behaviour of pyrrhotite [J]. International Journal of Mineral Processing, 2011, 98: 202−207.

[4] BEATTIE D A, HUYNH L, KAGGWA G B N, RALSTON J. The effect of polysaccharides and polyacrylamides on the depression of talc and the flotation of sulphide minerals [J]. Minerals Engineering, 2006, 19: 598−608.

[5] SHORTRIDGE P G, HARRIS P J, BRADSHAW D J, KOOPAL L K. The effect of chemical composition and molecular weight of polysaccharide depressants on the flotation of talc [J]. International Journal of Mineral Processing, 2000, 59: 215−224.

[6] BRAGA P F A, CHAVES A P, LUZ A B, FRANCA S C A. The use of dextrin in purification by flotation of molybdenite concentrates [J]. International Journal of Mineral Processing, 2014, 127: 23−27.

[7] KELEBEK S, YORUK S, SMITH W G. Wetting behavior of molybednite and talc in lignosuphonate/MIBC solutions and their separation by flotation [J]. Separation Science & Technology, 2006, 36: 145−157.

[8] ZHANG Wen-zheng. Progress of research on dressing technology of molybdenum ores [J]. China Molybdeunm Industry, 2009, 33: 1−6. (in Chinese)

[9] ZHANG Qi-dong, YUAN Zhi-tao, LIU Jiong-tian, LI Xiao-li, LU Ji-wei, LU Shuai-shuai. Effect of glucan on flotation separation of molybdenite and talc [J]. Chinese Journal of Nonferrous Metals, 2016, 26: 884−890. (in Chinese)

[10] YAN Hai-jun, LUO Xian-ping, ZHU Xian-wen, WENG Cun-jian, ZHANG Wen-pu, FENG Bo. Research progress on talc inhibitors in sulfide ore flotation [J]. Conservation and Utilization of Mineral Resources, 2020, 40: 138−144. (in Chinese)

[11] LI Ming-yang, WEI De-zhou, SHEN Yan-bai, LIU Wen-guang, GUO Shu-ling, LINAG Guo-qiang. Selective depression effect in flotation separation of copper–molybdenum sulfides using 2,3-disulfanylbutanedioic acid [J]. Transactions of Nonferrous Metals Society of China, 2015, 25: 3126−3132.

[12] FAN Xiao-hui, DENG Qiong, GAN Min, CHEN Xu-ling. Roasting oxidation behaviors of ReS_2 and MoS_2 in powdery rhenium-bearing, low-grade molybdenum concentrate [J]. Transactions of Nonferrous Metals Society of China, 2019, 29: 840−848.

[13] WANG Xing-jie, LIU Rui-zeng, MA Li-yuan, QIN Wen-qing, JIAO Fen. Depression mechanism of the zinc sulfate and sodium carbonate combined inhibitor on talc [J]. Colloids and Surfaces A: Physicochemical and Engineering Aspects, 2016, 501: 92−97.

[14] JENKINS P, RALSTON J. The adsorption of a polysaccharide at the talc–aqueous solution interface [J]. Colloids and Surfaces A: Physicochemical and Engineering Aspects, 1998, 139: 27−40.

[15] KHRAISHEH M, HOLLAND C, CREANY C, HARRIS P, PAROLIS L. Effect of molecular weight and concentration on the adsorption of CMC onto talc at different ionic strengths [J]. International Journal of Mineral Processing, 2005, 75: 197−206.

[16] MORRIS G E, FORNASIERO D, RALSTON J. Polymer depressants at the talc–water interface: Adsorption isotherm, microflotation and electrokinetic studies [J]. International Journal of Mineral Processing, 2002, 67: 211−227.

[17] WANG J, SOMASUNDARAN P, NAGARAJ D R. Adsorption mechanism of guar gum at solid–liquid interfaces [J]. Minerals Engineering, 2005, 18: 77−81.

[18] FENG Bo, JIAO Xiang-ke, WANG Hui-hui, PENG Jin-xiu, YANG Guang. Improving the separation of chalcopyrite and galena by surface oxidation using hydroxyethyl cellulose as depressant [J]. Minerals Engineering, 2021, 160: 106657.

[19] ZHONG Chun-hui, WANG Hui-hui, ZHANG Liang-zhu, GUO Meng-chi, FENG Bo. Flotation separation of molybdenite and talc by xanthan gum [J]. Powder Technology, 2021, 388: 158−165.

[20] NEJATIAN M, ABBASI S, AZARIKIA F. Gum Tragacanth: Structure, characteristics and applications in foods [J]. International Journal of Biological Macromolecules, 2020, 160: 846−860.

[21] CHEN Jian-hua, FENG Qi-ming. Current situation of molybdenam ore dressing [J]. Conservation and Utilization of Mineral Resources, 1994(6): 26−28. (in Chinese)

[22] WEI Zhen-lun, LI Yu-biao. Anisotropy of molybdenite surface and its effects on flotation mechanism [J]. Conservation and Utilization of Mineral Resources, 2018(3): 31−36. (in Chinese)

[23] LIN Qing-quan, GU Guo-hua, WANG Hui, LIU You-cai, WANG CHONG-qing, FU Jian-gang, ZHAO Jun-yao, HUANG Luo-luo. Recovery of molybdenum and copper from porphyry ore via iso-flotability flotation [J]. Transactions of Nonferrous Metals Society of China, 2017, 27: 2260−2271.

[24] LÜ Jian-ye, CHEN Yao-wen, ZHANG Heng-en. Flotation by change of molybdenite surface area and edge properties [J]. Multipurpose Utilization of Mineral Resources, 1992(1): 7−12. (in Chinese)

[25] GUO Wei, FENG Bo, PENG Jin-xiu, ZHANG Wen-pu, ZHU Xian-wen. Depressant behavior of tragacanth gum and its role in the flotation separation of chalcopyrite from talc [J]. Journal of Materials Research and Technology, 2019, 8: 697−702.

[26] ZHONG Chun-hui, FENG Bo, ZHANG Wen-pu, ZHANG Liang-zhu, GUO Yu-tao, WANG Tao, WANG Hui-hui. The role of sodium alginate in the flotation separation of apatite and dolomite [J]. Powder Technology, 2020, 373: 620−626.

[27] WANG Tao, FENG Bo, GUO Yu-tao, ZHANG Wen-pu, RAO Yu-bei, ZHONG Chun-hui, ZHANG Liang-zhu, CHENG Chen, WANG Hui-hui, LUO Xian-ping. The flotation separation behavior of apatite from calcite using carboxymethyl chitosan as depressant [J]. Minerals Engineering, 2020, 159: 106635.

[28] ZHOGN Chun-hui, WANG Hui-hui, FENGBo, ZHANG Liang-zhu, CHEN Yuan-gan, GAO Zhi-yong. Flotation separation of scheelite and apatite by polysaccharide depressant xanthan gum [J]. Minerals Engineering, 2021, 170: 107045.

[29] YI Hao, ZHAO Yun-liang, LIU Yi-ping, WANG Wei, SONG Shao-xian, LIU Chen, LI Hong-qiang, ZHAN Wen-quan, LIU Xin. A novel method for surface wettability modification of talc through thermal treatment [J]. Applied Clay Science, 2019, 176: 21−28.

[30] MIERCZYNSKA-VASILEV A, BEATTIE D A. The effect of impurities and cleavage characteristics on talc hydrophobicity and polymer adsorption [J]. International Journal of Mineral Processing, 2013, 118: 34−42.

[31] WALLQVIST V, CLAESSON P M, SWERIN A, SCHOELKOPF J, GANE P A C. Interaction forces between talc and hydrophobic particles probed by AFM [J]. Colloids and Surfaces A: Physicochemical and Engineering Aspects, 2006, 277: 183−190.

[32] SADEGHI S, RAD F A, MOGHADDAM A Z. A highly selective sorbent for removal of Cr(VI) from aqueous solutions based on Fe_3O_4/poly(methyl methacrylate) grafted Tragacanth gum nanocomposite: Optimization by experimental design [J]. Materials Science and Engineering C, 2014, 45: 136−145.

[33] KURT A. Physicochemical, rheological and structural characteristics of alcohol precipitated fraction of gum tragacanth [J]. Food and Health, 2018, 4: 183−193.

[34] KORA A J, ARUNACHALAM J. Green fabrication of silver nanoparticles by gum tragacanth (Astragalus gummifer): A

dual functional reductant and stabilizer [J]. Journal of Nanomaterials, 2012, 2012: 1−8.

[35] MONJEZI J, JAMALEDIN R, GHAEMY M, MOEINI A, MAKVANDI P. A performance comparison of graft copolymer hydrogels based on functionalized-tragacanth gum/polyacrylic acid and polyacrylamide as antibacterial and antifungal drug release vehicles [J]. International Journal of Nanotechnology and Nanomedicine, 2018, 1: 10−15.

[36] KHOSO S A, HU Yue-Hua, LÜ Fei, GAO Ya, LIU Run-qing, SUN Wei. Xanthate interaction and flotation separation of H_2O_2-treated chalcopyrite and pyrite [J]. Transactions of Nonferrous Metals Society of China, 2019, 29: 2604−2614.

黄薯树胶为抑制剂和丁基黄药为捕收剂的辉钼矿与滑石浮选分离

钟春晖[1]，冯 博[1,2,3]，陈渊淦[1]，郭梦池[1]，汪惠惠[1]

1. 江西理工大学 江西省矿业工程重点实验室，赣州 341000；
2. 矿冶科技集团有限公司 矿物加工科学与技术国家重点实验室，北京 102628；
3. 中南大学 战略含钙矿物资源清洁高效利用湖南省重点实验室，长沙 410083

摘　要：探索以黄薯树胶(TG)为抑制剂，实现辉钼矿与滑石的浮选分离。浮选试验表明，以丁基黄药(PBX)为捕收剂时，辉钼矿具有良好的可浮性，而滑石则被TG完全抑制，实现两种矿物的浮选分离。X射线光电子能谱(XPS)分析结果表明，TG以化学吸附的方式吸附在辉钼矿表面。接触角测试、傅里叶变换红外光谱(FTIR)和飞行时间二次离子质谱(ToF-SIMS)结果表明，TG在辉钼矿上的预先吸附不能阻止PBX在辉钼矿上的进一步化学吸附。由于PBX对滑石没有捕收能力，通过PBX捕收辉钼矿和TG抑制滑石实现辉钼矿与滑石的浮选分离。

关键词：辉钼矿；黄薯树胶；有机抑制剂；滑石；浮选分离

(Edited by Bing YANG)